# *FAULT LOCATION IN A VSC-HVDC LINK USING NEURAL NETWORKS*

Paula Páramo Balsa, Juan Manuel Roldán Fernández, Francisco González-Longatt, Manuel Burgos Payán y Jesús Riquelme Santos.

Universidad de Sevilla y University of South-Eastern Norway. Departamento de ingeniería eléctrica. Camino de los Descubrimientos, s/n, 41092, pparamo@us.es

Received: 14/Jan/2020 – Reviewing: 16/Jan/2020 -- Accepted: 27/Mar/2020 - DOI: http://dx.doi.org/10.6036/9637

*ABSTRACT:*

*High-voltage direct current (HVDC) using voltage source converter (VSC) in transmission systems applications are currently a competitive alternative to the traditional AC transmission systems, especially for offshore wind power applications. The increases of rated power and distance to the shore have made VSC-HVDC transmission systems economically more efficient than the conventional solution based on AC lines. Locating a fault in a submarine DC line must be fast and accurate because of the high cost of the submarine repairs as well as the operation cost (not-supplied energy). This paper proposed a fault location methodology based on artificial neural networks (ANN) for VSC-HVDC transmission system. The methodology only uses instantaneous values of electrical quantities (voltage and current) at one of the VSC terminal eliminating the problem of synchronisation. The proposed methodology has been tested and demonstrated using a typical VSC-HVDC test network, and simulation results show the appropriate performance of the methodology.*

*Keywords: Artificial Neural Networks, Fault Location, HVDC Transmission, VSC-HVDC*

## 1.- INTRODUCTION

Nowadays, the HVDC technology (*High Voltage Direct Current*) is in constant development [1]. This type of system is the most appropriate configuration to transport energy through long distances, since the rated power does is not limited by the distance in this type of lines [2], unlike the HVAC whose transport capacity decreases as the distance increases. Besides, the inductance in HVAC systems provokes phase lag between both terminals, causing instability in the system. This phenomenon does not occur in HVDC systems. Another advantage over HVAC systems is that DC systems allow connecting areas that function at different frequency [3]. In economic terms, an HVDC system has a lower cost of investment and greater efficiency for lines of high length [4]. Also, thanks to technological advances in power electronics, this technology is suitable for the synchronisation of renewable plants with the grid [5], including offshore wind farms. HVDC systems can be classified according to two main types of technologies: LCC (*Line Commutated Converter*), based on thyristors, and VSC (*Voltage Source Converter*), based on IGBTs. The last one is the most used nowadays due to its versatility, a lower rate of harmonic distortion and the capability to control active and reactive power [6], in contrast to the LCC which only controls active power [7]. Also, thanks to the improvement of the multilevel-modular VSC, LCC have not the advantage of efficiency anymore. However, the VSC-HVDC technology has disadvantages such as the complexity of the protection systems and their vulnerability to faults. The short-circuit current remains uncontrolled during a fault in DC. The current flows through the antiparallel diodes even when the IGBTs are opened, whereas, in case of thyristors, current can be cut off controlling the angle of fire [8]. Moreover, in long submarine DC cables, it is difficult to accurately estimate the location of a fault in order to repair it and restore the service. For this reason, the operation of these VSC-HVDC systems requires reliable, fast and accurate location methods to keep system stability [9]. Among all the existent methods of fault location, it should be mentioned (i) *method of travelling waves* and (ii) *failure analysis method*. The first method [10-11] is complicated because it requires much information about the dynamics of the current during the fault, and voltage sensors prepared for high frequencies. The second method is based on the system parameters and the electrical magnitudes during the fault. This one deal with the uncertainty of the electrical parameters of the system [12] and the de-synchronisation between the two measures at both terminals of the system.

This article proposes a methodology to estimate the location of a fault in a point-to-point-type bipolar VSC-HVDC system. The methodology is based on Artificial Neural Networks (ANN), which are fed with magnitudes of voltage and current during the transient of a fault. This technique has been used in many research works with very satisfactory results. However, one of the main problems of this type of networks is the complexity of the design process. There is not any guide about how to build an ANN, including all its parameters and key factors which must be considered for their calculation or estimation [13-17]. Artificial Intelligence, especially the neural networks, are demonstrating their effectiveness in several sectors of electrical engineering, despite being in the early stages of development in this field. For this reason, this paper has two objectives, firstly, estimating the location of a fault in a VSC-HVDC

system and secondly, the step-by-step design of the ANN, obtaining all its parameters, in order to facilitate the design of these algorithms to the researchers, and promote its penetration in the electrical engineering.

## 2.- MATERIAL AND METHODS

The ANN is an ideal tool for locating faults in VSC-HVDC systems, as they can model complex highly-nonlinear systems without a unique equation. The ANN is trained to learn a response based on several datasets of input and output data. The most extended ANN is the Multi-Layer Perceptron (MLP). The perceptrons in a layer of the MLP are entirely connected to the next one, and a weight ($w_i$) is associated with each connection. During the learning process, ANN is fed with a vector of inputs (p) and another with the desired outputs (a). Learning occurs when the weights of the connections are modified depending on the error at the output of the ANN in relation to the desired output. In the MLP, to obtain such errors, it is used the *backpropagation* algorithm. Once the ANN is trained, a new input can be introduced to obtain the estimation output. The proposed methodology is based on the selection of the training data, the creation of the ANN and the development of the training process of the ANN.

### 2.1.- TRAINING DATA

In this subsection, it is detailed the selection of the input vector of the ANN, (p), and the desired output vector (a).
For that purpose, the magnitudes of voltage and current have to be measured during a fault in the VSC-HVDC converting station: $V= [v_1, v_2, \ldots, v_{ns}]^T$ (1), $I= [i_1, i_2, \ldots, i_{ns}]^T$ (2) where *ns* is the number of samples in a time interval $\delta t$, at the sampling frequency $f_s$. It is important to remember that the values of voltage and current depend on the position, $x_i$, and the resistance, $R_f$, of the fault for the different training cases. Both vectors (1) and (2) compose the inputs vector, $p^x{}_{Rf} = [V^x{}_{Rf}\ I^x{}_{Rf}]^T$ (3), where the superscript *x* represents the positions of the faults considered, $x = [x_1, x_2, \ldots, x_n]^T$ (4), and $R_f$ represents the fault resistance, $R_f = [R_{f1}, R_{f2}, \ldots R_{fn}]^T$ (5). The desired output vector (a), represents the position of the fault, $a = x = [x_1, x_2, \ldots, x_n]^T$ (6).

### 2.2.- CREATION OF A ANN

The ANN is defined in terms of the number of neurons distributed on the layers, the connections, and the weights. The data is introduced in the *input layer*; it passes through the *hidden layer* and, finally, the product exits through the *output layer*. The ANN can be classified into (i) *Feed-forward (henceforth FF) and* (ii) *Feed-back (henceforth FB).* In FF networks, any output is an input of any neuronal unit of the same layer or layers above. The information only circulates from the neurons of the input layer toward the output. In FB networks, the outputs of the neurons can be inputs for units at the same or previous levels.
For this paper, FF networks have been implemented. They are classified as: *Feed-forward net* (FFN) and *Cascade-forward net* (CFN).

- In an FFN, the input is connected to a group of hidden layers which use a *sigmoid transfer function*. They are connected to an output layer which uses a linear function. Every neuron has a weight defined by the vector **w**; $\mathbf{w} = [w_{1,1}, w_{1,2}, \ldots, w_{1,R}]^T$ (7), **b** represents the bias and $\mathbf{n = w \cdot p + b}$ (8) the net inflow.
- CFN is similar to an FFN, except by an additional connection between the entrance and the output layer, without passing through the hidden layers.

Furthermore, it has been shown that any architecture similar to MLP requires a maximum of two hidden layers. In addition, since only one hidden layer is enough to obtain optimum results [18], only one will be used.
The inputs of the neurons have an associated weight which changes in the learning process. These weights are obtained iteratively so as the error is minimised. Nevertheless, in the previous step, it can happen an undesired phenomenon called *overfitting,* that causes the ANN memorises the training data. This would cause the loss of generalisation of the ANN and consequently the capacity to learn new cases. To avoid this, the input data is divided into: (i) *Training group*, (ii) *Validation group* and (iii) *Test group*. The first one is used to train the ANN and allows the weights to vary depending on their characteristics and values. The second group is used to adjust certain parameters associated with the training. The third one is used to check the reliability of the ANN for inputs which have not previously used.

## 2.3.- PROCESS OF TRAINING THE ANN

The selected training algorithm is *Levenberg-Marquardt,* as it is powerful and provides outstanding results [19]. In addition, it should be highlighted the use of the algorithm *backpropagation* (BP), based on the method of the gradient descent, due to its excellent performance on the resolution of complex problems. This algorithm has two stages: (i) *Learning forward,* and (ii) *Learning backwards.* In the first stage, the input patterns are in the first layer of the ANN, that spreads the values through all layers to the output. In the second stage, the obtained output and the desired one are compared, generating an error value for every neuron of the last layer. These errors are transmitted from the output layer to each one of the neurons of the intermediate layer. This process is repeated layer by layer until completing the whole network. Based on that error, the weights of each neuron are readjusted minimising the error. The function of the error to be minimised can be expressed in such a variety of ways, highlighting: (i) *Average quadratic error* (*MSE*), (ii) *Root of the mean square error* (*RMSE*) and (iii) *Mean absolute error* (MAE):

$$MSE = \frac{1}{2}\sum_{i=1}^{P}\sum_{j=1}^{M}\left(y_{ij} - t_{ij}\right)^2 \quad (9)$$

$$RMSE = \sqrt{MSE} \quad (10)$$

$$MAE = \frac{1}{2}\sum_{i=1}^{P}\sum_{j=1}^{M}\left|y_{ij} - t_{ij}\right| \quad (11)$$

Where $M$ is the number of variables and $P$ is the number of patterns. In addition, $y_{ij}$ is the $j$-th component of the desired output for the *i-th pattern*, and $t_{ij}$ the $j$-th component of the actual output for the *i-th pattern*.

The training method which has been implemented is the so-called *cross-validation*, due to the good practical results [20]. It consists in training the network $k$ =10 times, calculating the errors in each case and, subsequently, obtaining the global error. This method avoids the overfitting and, in consequence, the loss of generalisation.

## 3.- SIMULATION AND TRAINING OF THE ANN

The test system consists of a system of two VSC-HVDC converter stations, bi-polar type (± 640 kV), identified by the transmitter and receiver terminals, connected by a submarine 100-km-long cable per pole.

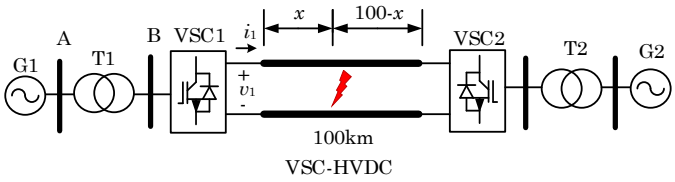


*Fig. 1. Test system.*

The system has the following parameters: DC power of 1000 MW, AC voltage (line-line) of 133 kV, DC voltage (line-line) of 640 kV DC, wire resistance of 0.0186 Ω/km, the inductance of the DC cable of 7.87641x10$^{-4}$ H/km, capacitance of the DC cable of 0.21 μF/km and frequency on the AC side of 50 Hz. The system has been developed using the software PSCAD, where EMT-type simulations of a phase-to-ground fault have been performed.

The input vector, $\mathbf{p^x_{Rf}} = [\mathbf{V^x_{Rf}}\ \mathbf{I^x_{Rf}}]^T$ (12), is a data window of 1.0 ms with a sampling frequency of 20 kHz, using voltage (**V**) and current (**I**) measured from a terminal. The input vector can be interpreted as a set of sub-vectors $\mathbf{p^x_{Rf}}$ where **x** represents the exact location of the fault and $\mathbf{R_f}$ the resistance of fault. The training values of $R_f$ are $\mathbf{R_f} = [0.0, 5.0, 10.0]^T$ Ω (13). For submarine lines, the $R_f$ values are low (iron or sea water between conductor and screen) [21-23].

The length of the input vector for each $R_f$ and x, is $2n \times 1$ = 401 samples. Faults every 1km along the whole line, so there are 99 vectors for each $R_f$ (297 vectors).

$$\begin{bmatrix} \overbrace{\begin{matrix} V_1^{L=1km} \\ \vdots \\ V_n^{L=1km} \end{matrix} \cdots \begin{matrix} V_1^{L=99km} \\ \vdots \\ V_n^{L=99km} \end{matrix}}^{R_f=0\Omega} & \overbrace{\begin{matrix} V_1^{L=1km} \\ \vdots \\ V_n^{L=1km} \end{matrix} \cdots \begin{matrix} V_1^{L=99km} \\ \vdots \\ V_n^{L=99km} \end{matrix}}^{R_f=5\Omega} & \overbrace{\begin{matrix} V_1^{L=1km} \\ \vdots \\ V_n^{L=1km} \end{matrix} \cdots \begin{matrix} V_1^{L=99km} \\ \vdots \\ V_n^{L=99km} \end{matrix}}^{R_f=10\Omega} \\ \begin{matrix} I_1^{L=1km} \\ \vdots \\ I_n^{L=1km} \end{matrix} \cdots \begin{matrix} I_1^{L=99km} \\ \vdots \\ I_n^{L=99km} \end{matrix} & \begin{matrix} I_1^{L=1km} \\ \vdots \\ I_n^{L=1km} \end{matrix} \cdots \begin{matrix} I_1^{L=99km} \\ \vdots \\ I_n^{L=99km} \end{matrix} & \begin{matrix} I_1^{L=1km} \\ \vdots \\ I_n^{L=1km} \end{matrix} \cdots \begin{matrix} I_1^{L=99km} \\ \vdots \\ I_n^{L=99km} \end{matrix} \end{bmatrix}_{2n\,x\,297} \quad (14)$$

The desired output vector contains the fault distances measured in per unit for every $R_f$ value; $\mathbf{a} = [x_{1/}\ell, x_{2/}\ell, \ldots x_{n/}\ell]^T$ (15). The first 99 items correspond to $R_f$ = 0 Ω, from 100th to 198th correspond to $R_f$ = 5 Ω, and the remaining values correspond to $R_f$ = 10 Ω.
Once the input vector and desired output vectors are created from PSCAD simulations results, for the development of the ANN is used *Matlab Neural Network Toolbox*.

The input data is divided into 237 vectors for training, 30 for validation and 30 for testing, avoiding overfitting of the ANN.

As there is no guide about how to calculate specific parameters of the ANN, it was decided to conduct several studies in order to obtain the number of hidden layers, the limits of training criteria (LCE) and the number of neurons per layer.

## 3.1. CALCULATION OF THE LIMITS OF TRAINING CRITERIA

These are going to be determined from the *correlation coefficient, R,* which establishes the proximity between the obtained and desired outputs. To calculate the number of neurons in the hidden layer, it is used *ad hoc* rules which, although not being mathematically justifiable, have demonstrated excellent results [18]. The *Rule of the geometric pyramid* sets the number of neurons for an unique hidden layer as: $N_c = \sqrt{N * M}$ (16), with *M* as the number of output neurons and *N* as the number of input variables. In this case, *N* = 40 and *M* = 1, it results as $N_C$ = 6.32. As it is not an exact value, the next integer values, by default and excess, are selected: 5, 6 and 7 neurons. From these, several tests are performed to calculate the LCE.

For this purpose, with an ANN with CFN structure and *Nc* = 6, the following steps are followed:

- Fixing the LCE to the default values set out by Matlab
- Training the ANN 10 times
- Checking the first of the ten training carried out, and determining for which of the five LCE the process has stopped
- Increasing the value of the LCE that has caused the stop
- Return to the second step

The criterion for finishing the loop is a maximum number of twelve iterations. The reason is that the time required by the ANN to be trained with very restrictive criteria is very high. Once all the steps have been done, the process is repeated for $N_C$ = {5, 7} and, similarly, for FFN.

Regarding the results, it can be seen that the ANN provides practically the same output in each training regardless of the LCE. The chosen LCE are: *Iterations=1000*, *Performance=0*, *Gradient=1.00x10-6* and *Number of checks=1000,* due to the lower simulation time consumption. Then, for which structure of ANN the correlation coefficients are closer to one and for which number of $N_C$ it happens. Thus, the best results are obtained from the configuration FFN, *Nc* = 5 and CFN, *Nc* = 6.

## 3.2. CALCULATION OF THE NUMBER OF NEURONS IN THE HIDDEN LAYER

The objective of this subsection is to check if the value of $N_C$ established in the previous subsection is correct, since the indexes *R* in some cases are similar. For this purpose, errors *MAE*, *MSE* and *RMSE* are calculated.

| | FFN | | | CFN | | |
|---|---|---|---|---|---|---|
| $N_c$ | 5 | 6 | 7 | 5 | 6 | 7 |
| MAE | **6.47x10$^{-4}$** | 7.07x10$^{-4}$ | 0.004 | 0.0256 | **0.0021** | 0.0043 |
| MSE | **3.00x10$^{-5}$** | 4.28x10$^{-5}$ | 0.0012 | 0.0016 | **1.86×10$^{-4}$** | 5.86×10$^{-4}$ |
| RMSE | **0.0055** | 0.065 | 0.0346 | 0.0400 | **0.0136** | 0.0242 |

*Table 1. MAE, MSE and RMSE errors according to structure and hidden neurons.*

The lowest errors have been obtained from the structures and *Nc* obtained on the previous sub-section; therefore, the values FFN, *Nc* = 5 and CFN, *Nc* = 6 are fixed.

## 3.3. RESULTS OF THE TRAINING OF THE ANN

Once all parameters have been established, the next step is to train the network applying the *cross-validation* method.
The following figures show the regression lines for each structure depending on $R_f$.

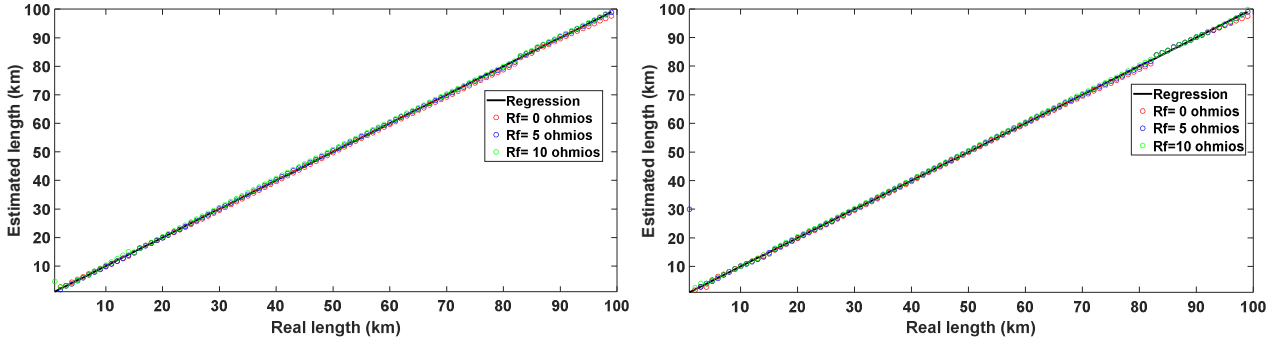


*Fig. 2. Regression line for FFN (left) and CFN (right).*

These lines establish the relation between the estimated and the actual length. Fig. 2 shows that, for all values of $R_f$, estimations are very close to the actual values. Thus, it has been demonstrated the power of the ANN created for each structure.
To check the robustness of the ANN, errors and correlation coefficients are calculated.

| *Errors* | | | | *Correlation coefficient* |
|---|---|---|---|---|
| *Structure* | *MSE (pu)* | *RMSE (pu)* | *MAE (pu)* | *R* |
| FFN | 5.453×10$^{-4}$ | 0.0234 | 0.0058 | 0.9965 |
| CFN | 0.0906 | 0.3009 | 0.0333 | 0.8730 |

*Table 2. Errors and correlation coefficient for both structures.*

Table 2 shows that the structure FFN provides the best estimations due to its lower errors and higher correlation coefficient.

### 3.3.1. ANN performance for noisy input signals

Trainings in the previous section use ideal signals, this means without considering the measurement error of the equipment (noise of a signal). Although it can be filtered, it is not possible to eliminate it completely. In this subsection, it is analysed the behaviour of the ANN when the input signals are altered with noise. This allows the analysis of the robustness and power of the ANN for each structure. A vector of noise $\boldsymbol{\Theta}(\mu,)$ is added to the input vector ($\mathbf{p}$). The noise vector is randomly generated with a gaussian distribution of average ($\mu$) zero and standard deviation $\sigma = \pm 1\%$. The new noisy signal ($\mathbf{p}^{\boldsymbol{\Theta}}$) is used for training for each structure and method.

After adding this noise, the errors and correlation coefficients are calculated.

| *Errors* | | | | *Correlation coefficient* |
|---|---|---|---|---|
| *Structure* | *MSE (pu)* | *RMSE (pu)* | *MAE (pu)* | *R* |
| FFN | 0.0305 | 0.1746 | 0.0289 | 0.9551 |
| CFN | 7.7335 | 2.7809 | 0.3050 | 0.7081 |

*Table 3. Errors and correlation coefficient for noisy inputs far both structures.*

As expected, the noise has led to an increase in the errors of both structures. For CFN a high increase in the errors is produced compared to Table 2, and therefore it does not provide reasonable estimations after disturbing the signal. This is also reflected in the correlation coefficient, which is further from the unit. However, in FFN case, the increment of the errors has been slight, and its correlation coefficient is still close to the unit. This way, it is demonstrated the power of the created ANN with FFN which, despite having modified its input, still provides very good estimations.

### 3.3.2. Adding new inputs to the trained ANN

The objective of this subsection is to determine the response of the ANN, previously trained with $R_f$ = [0, 5, 10] Ω, when new inputs are introduced. For this purpose, two scenarios are analysed:

- New input with $R_f$ close to the values used in the training process
- New input with $R_f$ distant from the values used in the training process

#### 3.3.2.1. New input with low Rf

Table 4 shows, the relative error of the estimation of the fault location according to $R_f$. Five locations (*x*) and six values of $R_f$ have been selected.

| *Location of the fault, x (km)* | *$R_f$ (Ω)* | | | | | |
|---|---|---|---|---|---|---|
| | *0* | *2.5* | *5* | *7.5* | *10* | *15* |
| 5 | 4.724 | 3.050 | 2.565 | 2.444 | 2.840 | 8.519 |
| 25 | 0.138 | 0.012 | 0.082 | 0.230 | 0.334 | 0.622 |
| 50 | 0.008 | 0.026 | 0.035 | 0.037 | 0.035 | 0.029 |
| 75 | 0.093 | 0.053 | 0.044 | 0.063 | 0.107 | 0.266 |
| 100 | 0.235 | 0.076 | $9.7 \times 10^{-5}$ | 0.019 | 0.034 | 0.373 |

*Table 4. Results of the % of relative error in the location of the fault.*

Results show that the higher $R_f$ the more significant errors. However, the ANN still provides reasonable estimates since these errors are not very high. It is important to note that, for $R_f$ values higher than 15 Ω, errors will gradually increase as the training have been conducted with $R_f$ = [0, 5, 10] Ω. In the case of submarine cable, the $R_f$ values are low, so the ANN with FFN structure provides reasonable estimates for new inputs with low $R_f$.

Even so, the response of the ANN for inputs with high $R_f$ is analysed. New inputs for fault resistances from $R_f$ = 0 Ω to $R_f$ = 100 Ω (increments of 2.5 Ω) are introduced. This way it is determined how it is affected the estimation of the ANN as $R_f$ reaches very different values from the training one. Fig. 3 shows estimations of the ANN according to RF for a real length of the fault of 75 km.

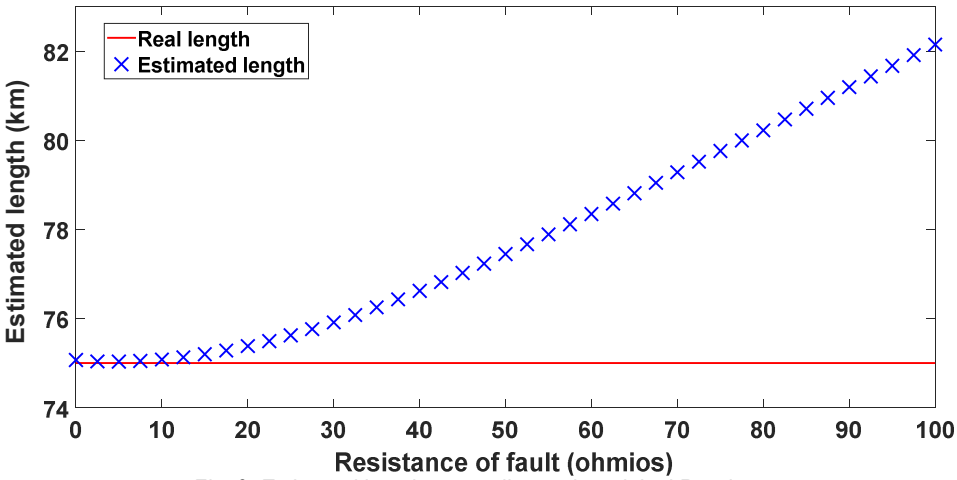


*Fig. 3. Estimated lengths according to the original $R_f$ value.*

In Fig. 3 It is noted that, the closer $R_f$ values to those used during practice, the closer estimations to the actual length.

### 3.3.2.2. New inputs with high $R_f$

In Fig. 3 it can be observed that, as the $R_f$ value of the new input increases, the estimated lengths gradually diverge from the actual length. Nevertheless, their relative errors are not high. For example, for $R_f$ = 50 Ω, the estimated length is 77.5 km. This means a relative error of 3.3 %. In the case of $R_f$ = 100 Ω, the estimated length is 82.15 km, which means a relative error of 9.5 %. Analysing these errors, the power of the ANN trained in this article is demonstrated, since it can achieve errors lower than 10 %, even when new inputs with values of $R_f$ far from those used during the training are added.

Finally, it is decided to carry out the last study to show that, depending on the data used for training, the obtained estimations will differ. For this purpose, a new ANN is created and trained in this subsection. The differences with respect to the ANN used throughout this research are the $R_f$ training values. In this ANN, the new input vector is composed of the voltage and current values for each location, x, now with $R_f$ = [75, 85, 100] Ω. Once trained, the response of the ANN for inputs with high $R_f$ is analysed. New inputs for fault resistances from $R_f$ = 0 Ω to $R_f$ = 100 Ω (increments of 2.5 Ω) are introduced. Fig. 4 shows the estimations of the new ANN according to $R_f$ for a real length of 75 km.

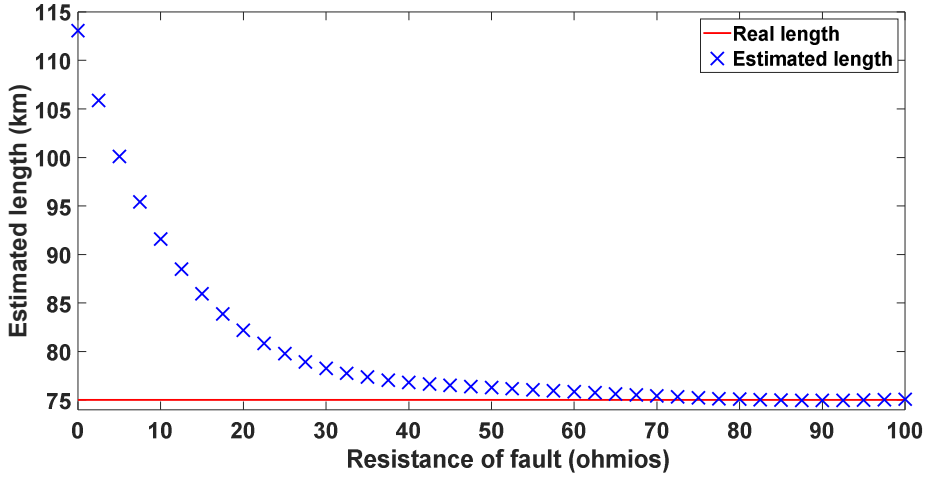


*Fig. 4. New Lengths estimated by the new ANN according to the $R_f$ value.*

Fig. 4 shows that for inputs with $R_f$ values close to those used during training, the estimations are very accurate.

## 4. CONCLUSIONS

This article provides a methodology for estimating the location of a fault in a VSC-HVDC system. For this purpose, several faults along the line are simulated with PSCAD in order to record voltage and current magnitudes. From these magnitudes, the vectors of inputs and desired output are built. Then the ANN is constructed using the Matlab Neural Network Toolbox. The calculation and selection of all its parameters are detailed. The chosen training method is *cross-validation*, with k=10 iterations, since this avoids overfitting of the network. In addition, a section has been added where the influence of the noise in signals is studied, as well as its effect on the regression lines and estimations. Without noise, both FFN and CFN structures present very good estimations, but FFN results are accurate. By disturbing with noise, CFN does not provide as reasonable estimates, while FFN still provides excellent results, demonstrating the power of the ANN with FFN. Furthermore, for different inputs from those used during training, the ANN provides satisfactory results, demonstrating its power. This has been tested for values between $R_f$ = 0 Ω and Rf = 15 Ω, as in submarine cables the $R_f$ that low.

Finally, the last case is studied, that reflects the importance of the training data setup according to the new inputs to estimate. It is demonstrated that the relative errors increase as the inputs differ from the data used during the training. In spite of that, errors remain below 10 %, which reflects the robustness of the ANN created.

## REFERENCES

[1] S. N. Martínez Lizana. "Análisis de Sistemas de Transmisión VSC-HVDC en Condición de Contingencia DC". Enrique López Parra, tut., Trabajo Fin de Máster para optar al grado de Máster en Ciencias de la ingeniería. Universidad de Concepción, Departamento de Ingeniería Eléctrica, Chile, 2019.

[2] L. F. Cayetano Cortés. "Estudio de planeación para sistemas de potencia, incluyendo enlaces de Corriente Directa en alta tensión, basado en pérdidas de potencia activa". Daniel Guillén Aparicio, tut., Trabajo Fin de Máster para optar al grado académico de Maestro en Ciencias. Tecnológico de Monterrey, Departamento de Ingeniería Eléctrica, Monterrey, 2019

[3] W. Aguirre Zambrano, L. A. Escobar Quishpe. "Estudio de las ventajas y desventajas de usar HVDC sobre sistemas de generación eólica". Diego Carrión, tut., Trabajo Fin de Carrera para optar al título de ingeniero eléctrico. Universidad Politécnica Salesiana, Quito, 2013

[4] J. Arrillaga, Y.H. Liu, N. R. Watson, "Flexible Power Transmission: The HVDC Options". John Wiley & Sons, Ltd. 2007.

[5] X. Zhang, N. Tai, X. Zheng, and W. Huang, "Wavelet-based EMTR method for fault location of VSC-HVDC transmission lines," J. Eng., vol. 2019, no. 16, pp. 961–966, 2019.

[6] M. Larruskain, I. Zamora, O. Abarrategui, A. Iturregi. "VSC-HVDC configurations for converting AC distribution lines into DC lines". *International Journal of Electrical Power & Energy Systems.* 54: 589 -597. 2014

[7] J. Yang, J.E. Fletcher, and J. O'reilly. "Short-circuit and ground fault analyses and location in VSC-based DC network cables". *IEEE Transactions on Industrial Electronics,* 59(10), pp. 3827-3837, 2012.

[8] O. E. Oni, I. E. Davidson, and K. N. I. Mbangula, "A review of LCC-HVDC and VSC-HVDC technologies and applications," EEEIC 2016 - Int. Conf. Environ. Electr. Eng., pp. 1–7, 2016.

[9] T. C. Peng, D. Tzelepis, A. Dysko, and I. Glesk, "Assessment of fault location techniques in voltage source converter based HVDC systems," 2017 IEEE Texas Power Energy Conf. TPEC 2017, 2017.

[10] M. N. Hashim, M. K. Osman, M. N. Ibrahim, A. F. Abidin, and M. N. Mahmud, "Single-ended fault location for transmission lines using traveling wave and multilayer perceptron network," Proc. - 6th IEEE Int. Conf. Control Syst. Comput. Eng. ICCSCE 2016, no. November, pp. 522–527, 2017.

[11] K. Hosseini, S. A. Tayyebi, and M. B. Ahmadian, "Double circuit transmission lines short circuit fault location using wavelet transform and MLP," 2017 25th Iran. Conf. Electr. Eng. ICEE 2017, pp. 1336–1342, 2017.

[12] Y. Liang, G. Wang, and H. Li, "Time-Domain Fault-Location Method on HVDC Transmission Lines Under Unsynchronised Two-End Measurement and Uncertain Line Parameters," *IEEE Transactions on Power Delivery,* vol. 30, pp. 1031-1038, 2015.

[13] A. Capar and A. B. Arsoy, "ANN fault location algorithms with high speed training," 2017 10th Int. Conf. Electr. Electron. Eng. ELECO 2017, vol. 2018-January, pp. 1360–1363, 2018.

[14] M. Dashtdar, R. Dashti, and H. R. Shaker, "Distribution network fault section identification and fault location using artificial neural network," 2018 5th Int. Conf. Electr. Electron. Eng. ICEEE 2018, pp. 273–278, 2018.

[15] N. Saravanan, and A. Rathinam "A comparitive study on ANN based fault location and classification technique for double circuit transmission line", *Proceedings - 4th International Conference on Computational Intelligence and Communication Networks, CICN 2012* 2012, pp. 824-830, 2012.

[16] S. K. Padhy, B. K. Panigrahi, P. K. Ray, A. K. Satpathy, R. P. Nanda, and A. Nayak, "Classification of Faults in a Transmission Line using Artificial Neural Network," Proc. - 2018 Int. Conf. Inf. Technol. ICIT 2018, pp. 239–243, 2018.

[17] Mohd Anuar Shafi'i; Noraliza Hamzah. "Internal fault classification using Artificial Neural Network", *4th International Power Engineering and Optimization Conference, PEOCO 2010,* pp. 352-357, 2010.

[18] R. Flores, and J.M. Fernandez. "Las redes neuronales artificiales: fundamentos teóricos y aplicaciones prácticas". Oleiros, La Coruña: Netbiblo. 9788497452465, 2008.

[19] J. Gracia, A. J. Mazón and I.Zamora. "Best ANN Structures for Fault Location in Single and Double-Circuit Transmission Lines". Power Delivery, IEEE Transactions on, vol. 20, no. 4, pp. 2389-2395, 2005.

[20] Mohd Anuar Shafi'i; Noraliza Hamzah. "Internal fault classification using Artificial Neural Network", 4th International Power Engineering and Optimization Conference, PEOCO2010, pp. 352-357, 2010.

[21] K. De Kerf, K. Srivastava, M. Reza, D. Bekaert, S. Cole, D. Van Hertem, et al., "Wavelet-based protection strategy for DC faults in multi-terminal VSC HVDC systems," Generation, Transmission & Distribution, IET, vol. 5, pp. 496-503, 2011.

[22] A. K. Khaimar and P. J. Shah, "Study of various types of faults in HVDC transmission system," Proc. - Int. Conf. Glob. Trends Signal Process. Inf. Comput. Commun. ICGTSPICC 2016, no. Lcc, pp. 480–484, 2017.

[23] T. Worzyk. "Submarine power cables: Design, installation, repair environmental aspects". Berlin: Springer-Verlag. 9783642012693, 2009.

## APPRECIATIONS

This work was partially supported by the Spanish MEC - Ministerio de Economía y Competitividad (Ministry of Economy and Competitiveness), co-funded by the European Commission (ERDF - European Regional Development Fund) under grant ENE2016-77650-R, as well as by the European Commission under grant SI-1778/12/2018. This work was also partially supported by grants US-1265887, Red CYTED 718RT0564 and CER-20191019.